Progress In Electromagnetics Research C, Vol. 13, 195–202, 2010

INTERACTION OF MEDICAL IMPLANTS WITH THE MRI ELECTROMAGNETIC FIELDS

S. A. Mohsin

University of Engineering and Technology
Lahore, Pakistan

J. Nyenhuis

Purdue University
West Lafayette, IN, USA

R. Masood

University of Engineering and Technology Lahore
Pakistan

Abstract—Medical implants in the form of linear conductive structures partially insulated along their length are especially prone to induced heating when subjected to the radiofrequency field used during magnetic resonance imaging (MRI). Leads or similar structures are often implanted near the skin and we have analyzed such implants when the implantation depth is varied in steps from 3 mm to 9 mm or more. Current, electric field, and induced temperature rise distributions in tissue have been obtained. The results have been validated by laboratory measurements.

1. INTRODUCTION

Lead devices implanted in body tissue are finding widespread use in interventional and therapeutic medicine. These include catheters, guide wires used during endovascular interventions, and lead devices that stimulate nerve or brain tissue by periodic pulses. For diagnostic purposes, patients often undergo magnetic resonance imaging (MRI). Vascular interventions are also often performed under MR guidance. Thus a quantitative investigation of the interaction of lead devices with

Corresponding author: S. A. Mohsin (syed_alimohsin@uet.edu.pk).

the MR electromagnetic fields is important. Two of the MR fields, the static magnetic field and the pulsed gradient fields do not show any appreciable interaction with an implant that does not contain any magnetic materials [1]. The main interaction is with the third field, the MR radiofrequency (RF) field. The scattered RF field that is produced causes heating of the tissue surrounding the implant. The tissue around the ends of implanted leads is especially prone to this RF — induced heating. This is due to the waveguiding effect that occurs in the insulation surrounding any long metal wire in a lead implant. Electromagnetic wave energy propagates in the insulation and is conveyed to the ends of the lead where it dissipated as heat in tissue. The temperature rises that result can be found by in-vitro measurements made in phantoms. Alternatively, electromagnetic fields can be computed using a numerical method such as the method of moments (MoM) [1, 2], or the finite difference time domain (FDTD) method [3, 4], or the finite element method (FEM) [5, 6]. Leads are often implanted below the skin and the implantation depth can vary. The present paper investigates the interaction of the MRI RF field with leads at various implantation depths, an aspect that has not been examined thoroughly before.

2. PLACEMENT OF THE LEAD IMPLANT AND FIELD COMPUTATION

The lead implant that has been used for simulation and measurement is shown in Figure 1. This implant has been proposed in a FDA standard [7], and serves as a benchmark implant for which results

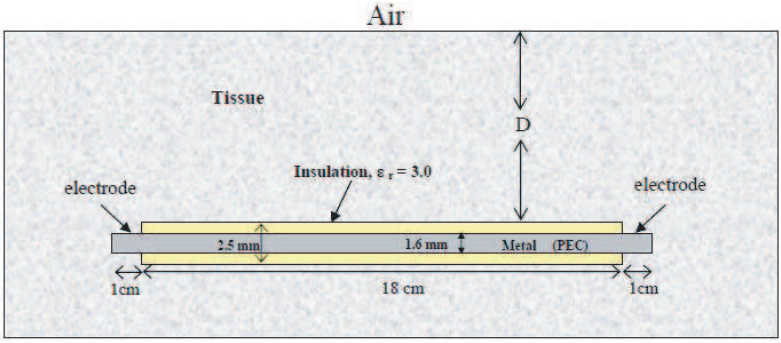

Figure 1. The model lead implant. The constitutive parameters of the embedding medium are $\sigma = 0.5\,\mathrm{S/m}$, $\varepsilon_r = 80$.

are widely available [4, 8]. It consists of a insulated metal wire with electrodes at the ends. The electrodes are typical of stimulation electrodes found at the ends of leads used for delivering pulses to brain or nerve tissue. The implant is embedded in muscle with $\sigma = 0.5\,\mathrm{S/m}$, $\varepsilon_r = 80$. The air-tissue interface is assumed to be planar. D is the perpendicular distance of the interface from the central axis of the implant. The behavior of the implant is examined for $D = 3$, 5, 7, and 9 mm. These are compared successively to each other and to the case for which D is ∞. These cases are solved for a 1.5 Tesla MRI system with $f = 64\,\mathrm{MHz}$. The background specific absorption rate (SAR) [1] in muscle is 2.5 W/kg which corresponds to a uniform RF field excitation of 100 V/m. The finite element method as outlined in [9, 10] is used for computing the scattered MRI radiofrequency field by solving the wave equation for the scattered electric field. Tetrahedral elements were used for the 3-D discretization. The metal was considered as a perfect electric conductor (PEC); the interior of the PEC was not part of the solution domain and only the surface of the PEC was meshed. The metal surface, the implant insulation, and a tissue layer immediately surrounding the implant was meshed much more finely than the rest of the domain. The finest meshing (no more than 0.3 mm $\times$0.3 mm) was used for the surface of the electrodes and the tissue adjacent to their surface. Comsol Mutiphysics has been used to obtain the field solutions.

3. THE CURRENT DISTRIBUTION IN THE IMPLANT AND THE ELECTRIC FIELD PRODUCED IN TISSUE

The magnitude of the current in the lead as a function of distance (along the lead) is shown in Fig. 2. Fig. 2(a) is the plot for a very deeply implanted lead, that is, D is ∞. Fig. 2(b) is the plot for $D = 7\,\mathrm{mm}$. All the current plots have the same overall shape as the current plot for infinite D case. However, there is a reduction in the current level as the value of D decreases (that is, the implant is moved closer to the skin). The peak current values for $D = 3$, 5, 7, and 9 mm have been found to be 84.5%, 89%, 92%, and 94% respectively of the peak current value for infinite D. The spatial electric field distribution for $D = 7\,\mathrm{mm}$ is shown in Fig. 3. Fig. 4 also shows a plot of the magnitude of the electric field as a function of distance along the lead; the plot is at a lateral distance of 0.2 mm from the metal surface and thus it shows the values of $|\mathbf{E}|$ at points in tissue adjacent to the bare metal electrode as well as in the insulation adjacent to the surface of the long metal connecting part. From 0 to 0.01 m and from 0.19 m to 2.0 m, the values of $|\mathbf{E}|$ are in tissue and from 0.01 to 0.19 m, the values are in the

insulation. The highest values of $|\mathbf{E}|$ are seen in the insulation, next to the proximal end of each electrode, but these high values do not pose a heating risk, since the insulation is almost a lossless dielectric. The current continuity equation along the lead implant is

$$\frac{dI}{dL} = -j\omega\rho_L = -j\omega 2\pi r_0 \rho_s \tag{1}$$

where I is the current in the lead implant at a distance L, r_0 is the radius of the bare metal cylinder, and ρ_L and ρ_s are the line and

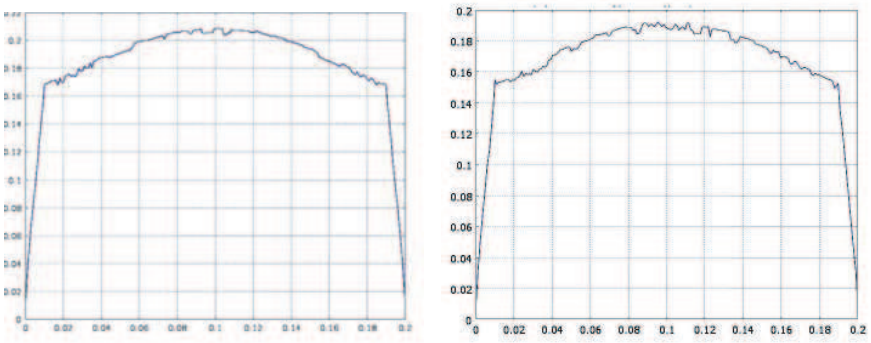

Figure 2. Magnitude of the current in the lead as a function of distance (y-axis in Amperes): (a) current plot for infinite D; (b) current plot for $D = 7\,\text{mm}$.

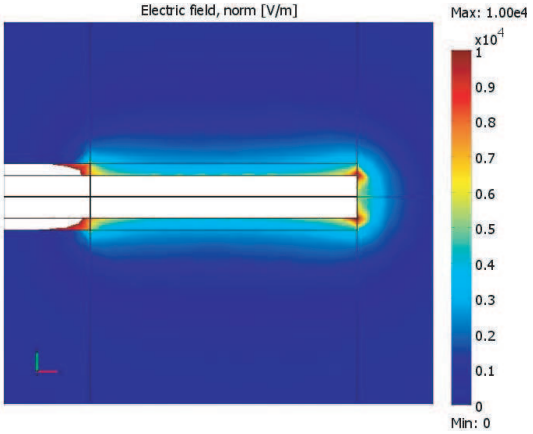

Figure 3. Spatial electric field (V/m) distribution for $D = 7\,\text{mm}$.

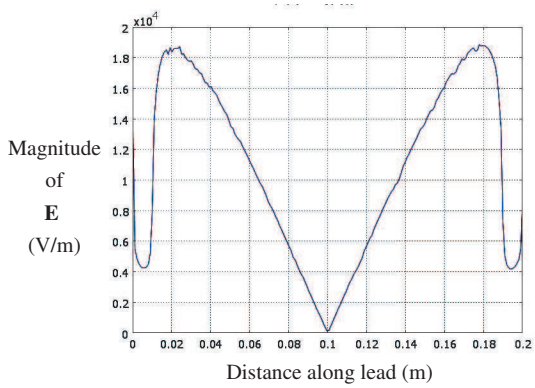

Figure 4. $|\mathbf{E}|$ along a line parallel to the implant surface (the line is at a lateral distance of 0.2 mm from the metal surface). Plot is for $D = 7$ mm. The electrodes are located from 0 to 0.01 m and from 0.19 m to 2.0 m.

surface charge densities respectively. $|\mathbf{E}|$ in Fig. 4 is not given exactly at the metal-tissue interface, but being only 0.2 mm away it reasonably approximates the value of $|\mathbf{E}|$ at the interface. At the electrode's surface, the total electric field must satisfy the boundary condition for the PEC-tissue interface,

$$\mathbf{E} = \frac{\rho_s}{\varepsilon_{tissue} - j\left(\sigma_{tissue}/\omega\right)}\widehat{n} \tag{2}$$

where ρ_s is the surface charge density and $\widehat{n}$ is the outward normal to the PEC surface. Eqs. (1) and (2) relate the slope of the current in Fig. 2(b) to the $|\mathbf{E}|$ values in Fig. 4.

4. TISSUE HEATING AND COMPARISON WITH LABORATORY MEASUREMENTS

Solving the bioheat equation [1] gives a spatial map of the temperature rise in the tissue surrounding the lead. The temperature has been solved for using FEM and Comsol Multiphsics. The temperature rise depends on the square of the electric field. The map for the infinite D case is shown in Fig. 5. The maximum temperature rise in tissue after 6 minutes of MR power is found to be 10.46°C. As D decreases, the temperature rise also decreases.

An important inference drawn from Eqs. (1) and (2) is that for two implants having the same current distributions, but one having a thinner metal core than the other, the electric field produced in

tissue will be higher around the thinner implant. As reported earlier in [11], significant temperature rises are produced in the brain tissue surrounding DBS leads; these are much higher than the temperature rises found here for the model implant. As can be seen from Eq. (1), ρ_s is greater on the electrodes of the DBS lead, since DBS leads are much thinner than the model implant. Then from Eq. (2), the electric field is more intense too.

Laboratory measurements were made with temperature probes in a phantom placed inside a MRI birdcage coil. Temperature rise on the model lead implant in multiple positions was measured to estimate the implantation depth effects. Temperature rise after 6 minutes was measured at the ends of the implant. Measurements were made for the lead placed at different distances from the wall of the phantom. The maximum value of the measured temperature rise (at the distal end of an electrode) for $D > 5\,\text{cm}$ and $D = 2\,\text{cm}$ was nearly 10°C in both cases. The corresponding measured values for $D = 9\,\text{mm}$ and $D = 3\,\text{mm}$ were 8.5°C and 6.4°C respectively. These results suggest that boundary effects on lead heating are minimal if the lead is at least 1 cm from the surface of the body.

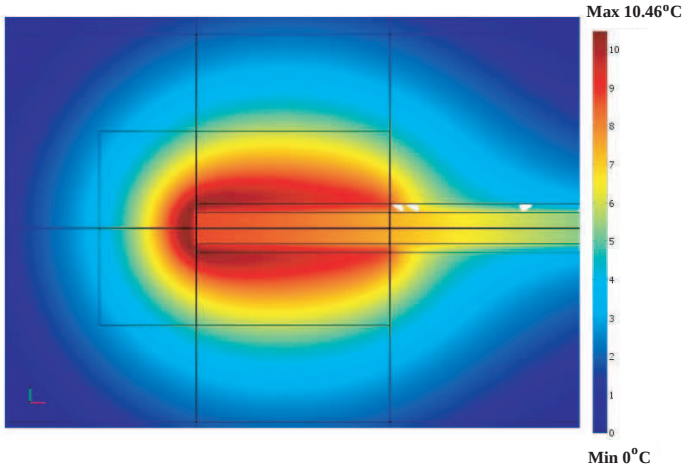

Figure 5. Spatial temperature rise distribution after 6 minutes of exposure to MR fields. This plot is for a very deeply implanted lead (D is taken to be infinite).

5. CONCLUSIONS

The MRI radiofrequency field heats tissue in the presence of implanted medical leads, especially around the bare metal electrodes at the ends of a lead. The heating effect is appreciable for an insulated lead because the insulation is like the dielectric between the two conductors of a coaxial transmission line, and an electromagnetic wave propagates in the dielectric. The heating effect is more for a deeply implanted lead, and as the implantation depth decreases, the heating effect also decreases. This is because of the fact that reflections from the tissue–air interface weaken the scattered RF field present in tissue around the lead. This boundary effect becomes almost zero when the implantation depth is 1 cm or more.

ACKNOWLEDGMENT

The first author gratefully acknowledges the cooperation of the MRI research group in the School of Electrical and Computer Engineering, Purdue University, West Lafayette, IN, USA during his research visit there.

REFERENCES

1. Nyenhuis, J. A., S. M. Park, R. Kamondetdacha, A. Amjad, F. G. Shellock, and A. Rezai, "MRI and implanted medical devices: Basic interactions with an emphasis on heating," *IEEE Trans. Device and Materials Reliability*, Vol. 5, No. 3, Sep. 2005.
2. Park, S. M., R. Kamondetdacha, A. Amjad, and J. A. Nyenhuis, "MRI safety: RF induced heating on straight wires," *IEEE Trans. Magn.*, Vol. 41, No. 10, 4197–4199, Oct. 2005.
3. Ho, H. S., "Safety of metallic implants in magnetic resonance imaging," *J. Magn. Reson. Imag.*, Vol. 14, 472–474, 2001.
4. Amjad, A., "Specific absorption rate during magnetic resonance imaging," Ph.D Thesis, Purdue University, 2007.
5. Mohsin, S. A., N. M. Sheikh, and U. Saeed, "MRI-induced heating of deep brain stimulation leads," *Phys. Med. Biol.*, 5745–5756, 2008.
6. Jin, J. M., J. Chen, W. C. Chew, H. Gan, R. L. Magin, and P. J. Dimbylow, "Computation of electromagnetic fields for high-frequency magnetic resonance imaging applications," *Phys. Med. Biol.*, Vol. 41, 2719–2738, 1996.

7. Kainz, W., "SAR intercomparison protocol for 1.5 T MR systems draft," U.S. Food and Drug Administration, Center for Devices and Radiological Health, Office of Science and Engineering Laboratories, 2006.
8. Park, S.-M., R. Kamondetdacha, and J. A. Nyenhuis, "Calculation of MRI-induced heating of an implanted medical lead wire with an electric field transfer function," *J. Magn. Reson. Imag.*, Vol. 26, 1278–1285, 2007.
9. Volakis, J. L., A. Chatterjee, and L. C. Kempel, "Review of the finite-element method for three-dimensional electromagnetic scattering," *J. Opt. Soc. Am. A*, Vol. 11, No. 4, Apr. 1994.
10. Jin, J., *The Finite Element Method in Electromagnetics*, 2nd Edition, Chaps. 5, 8, and 9, John Wiley and Sons, 2002.
11. Mohsin, S. A., N. M. Sheikh, and U. Saeed, "MRI induced heating of deep brain stimulation leads: Effect of the air-tissue interface," *Progress In Electromagnetics Research*, PIER 83, 81–91, 2008.